ELSEVIER

Pump-probe spectra and nuclear dynamics for a dissipative molecular system in a strong laser field: predissociation dynamics

Yutaka Maruyama, Yoshitaka Tanimura

The Graduate University for Advanced Studies and Institute for Molecular Science, Myodaiji, Okazaki 444-8585, Japan

Abstract

The predissociation dynamics of a molecular system under a strong laser field in the condensed phase is investigated by direct numerical integration of the multi-state quantum Fokker-Planck equation. Numerical calculations of probe absorption spectra driven by a strong pump pulse are presented, and discussed. The results show dynamical Stark splitting, but, in contrast to the Bloch equations which contain an infinite-temperature dephasing, we find that at finite temperatures their peaks have different heights even when the pump pulse is on resonance. Furthermore we observe the effect of the diabatic coupling between excited and dissociative states as the peaks on the spectra. © 1998 Published by Elsevier Science B.V. All rights reserved.

1. Introduction

Progress in ultrafast experimental techniques propel not only the linear but also the nonlinear spectroscopy, which provide a direct means for studying nuclear dynamics in the condensed phase. Further the laser techniques become to allow high intensity and short pulse. One of the central questions is whether the interaction between the high-intensity electromagnetic field and the molecule gives rise to new phenomena which do not occur under ''normal'' conditions, i.e. low intensities and large pulse durations [1–4].

On the other hand, the predissociation, caused by curve crossing between bound and dissociative states, is interesting phenomenon. Photoinduced dissociation and chemical reaction connect to this phenomenon directly and are studied extensively [5–8].

In the previous study we calculated the pump-probe spectra for displaced harmonic and Morse oscillators system in the strong laser field using the multi-state Fokker-Planck equation for a Gaussian-Markovian noise bath [9,10]. The results showed the effect of finite temperature as well as anharmonicity of a potential, which would not be obtained from the optical Bloch equation [11,12] or the stochastic Liouville equation [13] approach. In this paper, we investigate the probe absorption spectra for a Morse potentials system with a dissociative state in a strong laser field. Our aim is to observe the effect of diabatic coupling between the excited and dissociative states under the strong laser field.

2. Pump-probe spectroscopy

We consider a molecular system with electronic states denoted by $|j\rangle$. The Hamiltonian of the system is

$$H_S = \frac{p^2}{2M} + \sum_j \sum_k |j\rangle U_{jk}(q)\langle k|. \qquad (1)$$

Here, q is a nuclear coordinate strongly coupled to the electronic state and p is its conjugate momentum. The diagonal element $U_{jj}(q)$ is the potential surface of the jth electronic surface, and the off-diagonal element $U_{jk}(q)$ with $j \neq k$ represents the diabatic coupling between the jth and the kth states. In this paper, we study a pump-probe experiment in a three-level system with Morse potential surfaces denoted by $|g\rangle$, $|e\rangle$ and $|e'\rangle$ (Fig. 1). The transition frequency between g and e is denoted by ω_{ge}. We assume that the system is initially in the ground equilibrium state $\rho = |g\rangle \rho_g \langle g|$, where ρ_g is the equilibrium distribution function of the ground potential surface. In pump-probe experiment, the system is subjected to two light pulses: a strong pump and a weak probe whose frequencies and wave vectors are denoted by Ω_1, k_1 and Ω_2, k_2, respectively. We assume that Ω_1 and Ω_2 are close to the electronic transition frequency between g and e. The total Hamiltonian in the rotating wave approximation is then given by

$$H_A(t) = H_S + E_1(t)\left(e^{ik_1 r - i\Omega_1 t}\mu_1^+ + e^{-ik_1 r + i\Omega_1 t}\mu_1^-\right)$$
$$+ E_2(t)\left(e^{ik_2 r - i\Omega_2 t}\mu_2^+ + e^{-ik_2 r + i\Omega_2 t}\mu_2^-\right), \tag{2}$$

where $E_1(t)$ and $E_2(t)$ are the temporal envelopes of the pump and probe pulses, $\mu_1^+ = \mu|e\rangle\langle g|$ and $\mu_1^- = \mu|g\rangle\langle e|$ are the dipole operators of pump pulse and $\mu_2^+ = \mu|e\rangle\langle g|$ and $\mu_2^- = \mu|g\rangle\langle e|$ are ones of probe pulse. In order to calculate probe absorption spectra, we employed the following procedure [9,10]. First
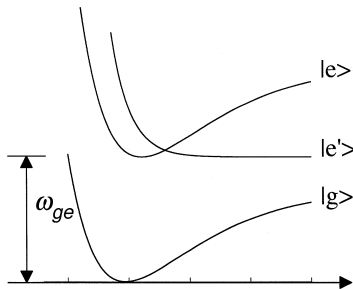

Fig. 1. Potential surfaces of the displaced Morse oscillators system with the dissociative state. The resonant frequency between $|g\rangle$ and $|e\rangle$ is expressed by ω_{ge}.

we consider the evolution of the system subject only to the pump field. The Hamiltonian is then given by

$$H_A^0(t) = H_S + E_1(t)\left(e^{ik_1 r - i\Omega_1 t}\mu_1^+ + e^{-ik_1 r + i\Omega_1 t}\mu_1^-\right). \tag{3}$$

The corresponding solution of the Liouville equation is denoted $\rho^0(t)$:

$$\frac{d}{dt}\rho^0(t) = -\frac{i}{\hbar}\left[H_A^0(t), \rho^0(t)\right]. \tag{4}$$

We next introduce a modified Hamiltonian which includes only the negative frequency component of the probe pulse E_2

$$H_A'(t) \equiv H_A^0(t) + E_2(t) e^{-i\Omega_2 t}\mu_2^+. \tag{5}$$

The solution of the Liouville equation with this Hamiltonian will be denoted $\rho'(t)$:

$$\frac{d}{dt}\rho'(t) = -\frac{i}{\hbar}\left[H_A'(t), \rho'(t)\right]. \tag{6}$$

If we expand $\rho'(t)$ to first order in the probe, we obtain

$$P_{k_2}(t) \approx 2\,\mathrm{tr}\left\{\mu_2^-\left(\rho'(t) - \rho^0(t)\right)\right\}$$
$$= -i\int_{-\infty}^{t} dt'\, E_2(t')$$
$$\times e^{-i\Omega_2 t'}\langle\left[\mu_2^-(t), \mu_2^+(t')\right]\rangle + \dots . \tag{7}$$

The above expression agrees with the intensity of the probe absorption. We can thus calculate the probe absorption with the frequency ω_2 by subtracting two solutions of the Liouville equation, which can be expressed in the form

$$S(\omega_2) = -\sqrt{\frac{8}{\pi}}\,\mathrm{Im}\left\{E_2[\omega_2]\right.$$
$$\left.\times \int dt\, e^{i\omega_2 t} tr\left[\mu_2^-\left(\rho'(t) - \rho^0(t)\right)\right]\right\}, \tag{8}$$

where $E_2[\omega_2]$ is the Fourier transform of the probe field amplitude. This scheme can be applied to a system driven by pump pulses of arbitrary number, shape, and strength.

3. Quantum Fokker-Planck equation for a multi-state system interacting with a Gaussian-Markovian noise bath

We now include an environment consisting of a set of harmonic oscillators with coordinates x_n and momenta p_n. The interaction between the system and the nth oscillator is assumed to be linear with a coupling strength c_n. The total Hamiltonian is then given by

$$
H(t) = H_A(t)
$$
$$
+ \sum_n \left[\frac{p_n^2}{2m_n} + \frac{m_n \omega_n^2}{2} \left(x_n - \frac{c_n q}{m_n \omega_n^2} \right)^2 \right].
$$
$$(9)$$

The character of the heat-bath is specified by the spectral distribution: All information about the bath which is required for a reduced description of the system dynamics, is contained in its initial temperature and its spectral density. We assume the Ohmic dissipation with the Lorentzian cutoff,

$$
J(\omega) = \frac{M\zeta}{2\pi} \frac{\omega \gamma^2}{\gamma^2 + \omega^2}.
$$
$$(10)$$

With the assumption of the high temperature bath $\beta \hbar \gamma \leq 1$, this spectral density represents a Gaussian-Markovian noise where the symmetric correlation function of the noise induced by the heat-bath, is proportional to $M\zeta\gamma\, e^{-\gamma t}/\beta$. Thus, ζ and γ correspond to the friction and the relaxation time of the noise, respectively. In this case, one can trace over the heat-bath degrees of freedom and obtain the equation of motion in the hierarchy form [14–16]. The important point is that the restriction does not involve the system characteristics frequencies (which can be small or large compared to β^{-1}), but only a high temperature requirement with respect to the bath parameters, which is much easier to meet. In the following, we employ the Wigner distribution [17,18] defined by

$$
W_{jk}(P,R;t)
$$
$$
= \frac{1}{2\pi\hbar} \int_{-\infty}^{\infty} dr\, e^{iPr/\hbar} \rho_{jk}(R - r/2, R + r/2; t).
$$
$$(11)$$

For the nth member of hierarchy, $W_{jk}^{(n)}$, where j and k represent diabatic states, the equation of motion is expressed as [19]

$$
\frac{\partial}{\partial t} W_{jk}^{(n)}(P,R;t)
$$
$$
= -\frac{P}{M} \frac{\partial}{\partial R} W_{jk}^{(n)}(P,R;t) - \frac{1}{\hbar} \int \frac{dP'}{2\pi\hbar}
$$
$$
\times \sum_m \Big[X_{jm}(P - P', R; t) W_{mk}^{(n)}(P', R; t)
$$
$$
+ X_{mk}^*(P - P', R; t) W_{jm}^{(n)}(P', R; t) \Big]
$$
$$
- n\gamma W_{jk}^{(n)}(P,R;t) + \frac{\partial}{\partial P} W_{jk}^{(n+1)}(P,R;t)
$$
$$
+ n\zeta\gamma \left(P + \frac{M}{\beta} \frac{\partial}{\partial P} \right) W_{jk}^{(n-1)}(P,R;t),
$$
$$(12)$$

and anchor equation for large N ($N\gamma \geq \omega_0$: ω_0 is the characteristic frequency of the system)

$$
\frac{\partial}{\partial t} W_{jk}^{(N)}(P,R;t)
$$
$$
= -\frac{P}{M} \frac{\partial}{\partial R} W_{jk}^{(N)}(P,R;t) - \frac{1}{\hbar} \int \frac{dP'}{2\pi\hbar}
$$
$$
\times \sum_m \Big[X_{jm}(P - P', R; t) W_{mk}^{(N)}(P', R; t)
$$
$$
+ X_{mk}^*(P - P', R; t) W_{jm}^{(N)}(P', R; t) \Big]
$$
$$
- N\gamma W_{jk}^{(N)}(P,R;t)
$$
$$
+ \zeta \frac{\partial}{\partial P} \left(P + \frac{M}{\beta} \frac{\partial}{\partial P} \right) W_{jk}^{(N)}(P,R;t)
$$
$$
+ N\zeta\gamma \left(P + \frac{M}{\beta} \frac{\partial}{\partial P} \right) W_{jk}^{(N-1)}(P,R;t).
$$
$$(13)$$

Here, ζ is the friction constant and

$$
X_{ij}(P,R;t) = i \int dr\, e^{iPr/\hbar} U_{ij}(R - r/2; t),
$$

$$
X_{ij}^*(P,R;t) = -i \int dr\, e^{iPr/\hbar} U_{ij}(R + r/2; t)
$$
$$(14)$$

are the Fourier transform representation of the potential terms.

4. Numerical calculation

We consider the displaced Morse potentials system with the dissociative state defined by (see Fig. 1);

$$U_{gg}(R) = E_e\{1 - e^{-a(R-D_1)}\}^2,$$

$$U_{ee}(R) = E_e\{1 - e^{-a(R-D_2)}\}^2 + \hbar\omega_{ge},$$

$$U_{e'e'}(R) = E_e e^{-2a'(R-D_2)} + \hbar\omega_{ge},$$

$$U_{ee'}(R) = A \tag{15}$$

where E_e, a and D_j are the dissociation energy, the curvature of the potential and the displacement, respectively. The excited state e is coupled diabatically to the dissociative state by constant force.

Hereafter, we employed the dimensionless coordinate and momentum defined by $r = R\sqrt{M\omega_0/\hbar}$ and $p = P\sqrt{1/M\hbar\omega_0}$, respectively, where $\omega_0 = \sqrt{U''_{gg}(R)/M}$. The displacement and curvature of the potential, D_1, D_2, a, etc. are also measured in this unit. We set $E_e = 3649.5$ cm^{-1}, $a = 0.6361$ and $D_1 = 40.598$ as the ground state of Cs_2 molecule [20,21], which has been studied by a variety of spectroscopic experiments. The fundamental frequency is then given by $\omega_0 = 38.7$ cm^{-1}. We calculate probe absorption spectra for the displacement $D_2 = 43.598$. For the dissociative state, the parameters were chosen to be $d' = 0.6361$ and $A = 300$ cm^{-1}, respectively. We have used the value of friction $\zeta = 0.16$ cm^{-1}, the inverse correlation time $\gamma = 4.8$ cm^{-1}, and the initial temperature $T = 300$ K, which satisfies the condition $\beta\hbar\gamma = 0.023 \ll 1$.

We first calculate the initial equilibrium state by integrating the equation of the motion from time $t = -t_i$ to $t = 0$ with the temporally initial condition,

$$W_{gg}^{(0)}(p,r;-t_i) = \exp\left[-\beta\left(\hbar\omega_0 p^2/2 + U_{gg}(r)\right)\right],$$

$$W_{gg}^{(n)}(p,r;-t_i) = 0. \tag{16}$$

Note that Eq. (16) is the equilibrium state of the system itself, but, it is not the equilibrium state of the total system, since it neglects the system-bath initial correlation, but we can obtain to ''true'' equilibrium state at $t = 0$, if we set $|t_i|$ for a sufficiently

longer time than the characteristic time of the system [15].

The numerical integration of the kinetic equations was performed by using second-order Runge-Kutta method for finite difference expressions of the momentum and the coordinate space. The size of grid was chosen to be 70×501 in the mesh range $-17 < p < 17$ and $33 < r < 78$. We have taken into account $N = 11$ hierarchy elements for $W^{(n)}$. We calculate the pump-probe spectra by integrating the equation of motion (12) and (13) instead of the Liouville equation following the procedure explained in Section 2.

We assume that pump and probe pulses are Gaussian

$$E_1(t) = \theta_1 \exp\left[-(t/\tau_1)^2\right],$$

$$E_2(t) = \theta_2 \exp\left[-(t-\tau)^2/\tau_2^2\right], \tag{17}$$

with resonance central frequencies, i.e., $\Omega_1 = \Omega_2 = \omega_{ge}$. We measure the transition between the $|g\rangle$ and $|e\rangle$ states only. The pulse durations were taken to be $\tau_1 = 700$ fs and $\tau_2 = 30$ fs and the time delay was varied between $\tau = -2.0$ ps and $\tau = 1.0$ ps, i.e., the pump and the probe pulse are overlapped. The pump intensity was $\mu\theta_1 = 4.77$ THz and the probe was weak $\mu\theta_2 = 1.59$ GHz. Considering ideal gas with pressure of 1 atm at 300 K, they are equivalent to 3.14×10^6 W/m^2 and 1.05×10^3 W/m^2, respectively, for the dipole moment $\mu = 1$ Debye.

In Fig. 2, we show the pump-probe spectra for the strong pulse excitation. The solid lines denote the spectra in the present predissociation case. To see the effects of the dissociative state, we also display the same results without the dissociative state which were given in Ref. [10] (the dashed lines). We set $\triangle\omega = \omega - \omega_{ge}$. The spectrum at $\tau = -2.0$ ps is similar to the linear absorption spectrum, since the pump is weak and its effects are small at this early stage. The vibronic side-band peaks are observed in the probe absorption spectrum corresponding to various vibronic absorption-emission processes. The peak about -380 cm^{-1} is attributed to the movement of the wavepacket during nonimpulsive probe detection. The curves at $\tau = -1.5$ and $\tau = -1.0$ ps show the dips about 0 cm^{-1} caused by the unbalance between the population and the coherent contribution of an

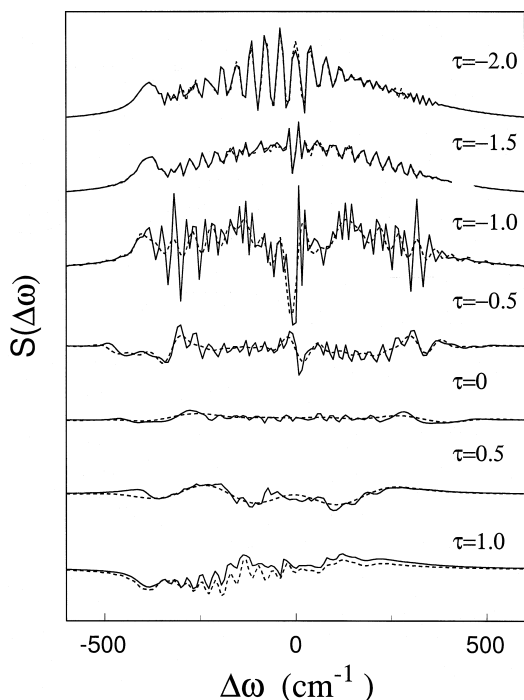Fig. 2. Pump-probe spectra for a strong excitation ($\mu\theta_1 = 4.77$ THz) for different pulse delays τ (ps). The solid (dashed) lines show the spectra for the system with (without) diabatic coupling case. We set $\Delta\omega = \omega - \omega_{ge}$.

absorption spectrum (the coherent dips) [22]. In the previous case (dashed lines), when the pump pulse becomes stronger, the coherent dips are broadened. Each vibronic transition shows a Stark splitting whose magnitude is given by the proper Rabi frequency $\Delta\Omega_{nm} = \sqrt{\Delta\omega_{nm}^2 + (\mu E_1(t))^2}$, where $\Delta\omega_{nm}$ is the energy difference between the nth vibrational state of U_{gg} and the mth vibrational state of U_{ee}. The Stark peak of the origin ($\Delta\omega = 0$), which corresponds to the zero vibronic line then splits to the blue and to the red. At $\tau = -1.0$ ps the spectrum shows many peaks in comparison with the non-dissociative case depicted by the dashed line. This is understandable through the following argument. The diabatic coupling between the e and e' states causes the additional vibrational levels to the excited states around the energy at the crossing point. Since the laser interacts only between the g and e states, such additional levels are dark for the laser excitation. Therefore at the beginning of the pump excitation

($\tau < -1.5$ ps), these dark levels do not play any role, and the probe absorption in the displaced Morse oscillators (dashed lines) and the displaced Morse oscillators with the dissociative state case (solid lines) show similar results. At time $\tau > -1.0$ ps, if the dissociative state is exist, some population in the e state transfers into the dark levels through the diabatic coupling as predissociation. Such reduction of population in the e states induces the additional excitation from the g to e state, which appears as many new peaks in the absorption spectra. For $\tau = 1.0$ ps, the pump excitation becomes weak enough and the structure of vibronic bands is recovered.

Fig. 3 shows the time-evolution of the wavepackets $W_{gg}(p,r;t)$, $W_{ee}(p,r;t)$, and $W_{e'e'}(p,r;t)$. In each figure, the upper one is for $|e\rangle$ (the excited state), the middle one is for $|e'\rangle$ (the dissociative state), and the lower one is for $|g\rangle$ (the ground state). At $\tau = -1.5$ ps when the pump pulse is weak, the wavepacket is close to the shape of the ground equilibrium state. Since we considered the Gaussian (non impulsive) laser excitation, the wavepacket goes up and down between the ground and excited state potentials through the laser interaction, therefore the shape of the ground state wavepacket is also changed. For $\tau = -1.0$ ps, the population of the excited state increases due to the strong pump pulse, and the population transfer from the g to e state takes place more quickly than that of the non-dissociative state case. The wavepacket created in the e state is forced by the potential and moves in the positive coordinate direction. At the $\tau = -0.5$ ps the wavepacket reaches and passes the curve crossing point (about $r = 52$). Although we have used a coordinate independent diabatic coupling, the transition mainly takes place in the vicinity of the curve crossing point, and the e' population suddenly increases when the e state wavepacket passes the crossing point. This is because of the potential difference between e and e' states $\delta U(r) = |U_{ee}(r) - U_{e'e'}(r)|$. The off-diagonal elements $W_{ee'}$ and $W_{e'e}$ are highly oscillatory functions of time at positions far from the curve crossing point, where $\delta U(r)$ is large. Thus, $W_{e'e'}$ can be large only near the crossing point, where $\delta U(r)$ is small [19]. After passing the crossing point, the transferred wavepacket starts to move in the e' state potential surface. Since the wavepacket in the e' potential is not stable, the wavepacket in the e' state quickly
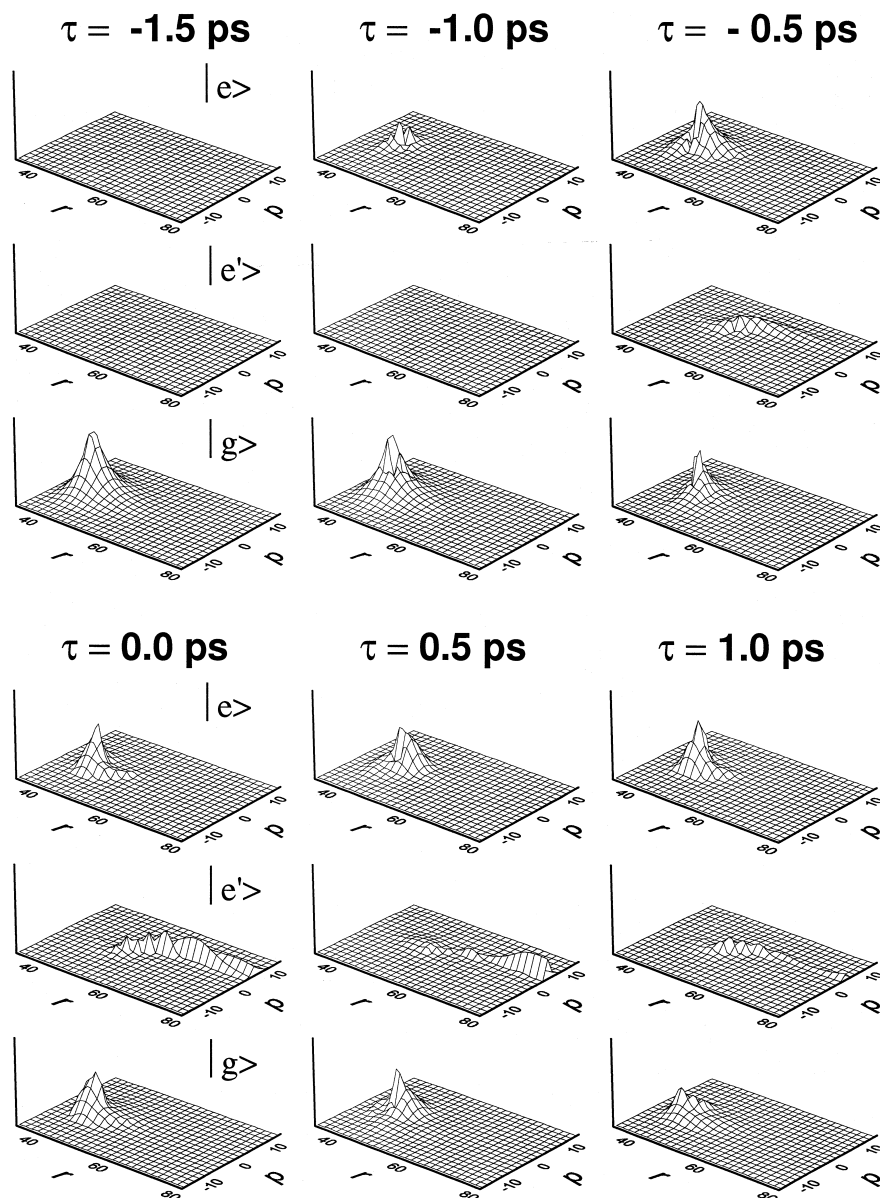
$\tau = $ -1.5 ps $\tau = $ -1.0 ps $\tau = $ - 0.5 ps

$|e\rangle$

$|e'\rangle$

$|g\rangle$

$\tau = $ 0.0 ps $\tau = $ 0.5 ps $\tau = $ 1.0 ps

$|e\rangle$

$|e'\rangle$

$|g\rangle$

Fig. 3. The time-evolution of the wavepackets of the ground ($|g\rangle$), excited ($|e\rangle$) and dissociative ($|e'\rangle$) states for strong pump excitation. In each figure, the upper one is for $|e\rangle$, the middle one is for $|e'\rangle$, and the lower one is for $|g\rangle$.

moves to the positive ($\tau = -0.5$ ps) and then goes out from the edge of potential ($\tau = 0.0$ ps). Compare with the non-dissociative case, at $\tau = 0.0$ ps, the positive momentum parts of the wavepackets on g

and e are small due to predissociation. For $\tau = 0.0$, 0.5 and 1.0 ps, the populations on g and e states slightly decreases and increases because of Rabi flopping, and the wavepackets oscillate on each po-

tential surfaces. After the pump pulse is vanished, those wavepackets will reach to the thermal equilibrium state of each potential surface after long time.

5. Conclusion

In this paper we calculate the pump-probe spectra and nuclear dynamics for a displaced Morse oscillators system with the dissociative state by using multi-state quantum Fokker-Planck equation for a Gaussian Markovian bath. The results show interplay between vibronic transitions and dynamical Stark splitting, and denote the effect of diabatic coupling between bound and dissociative states. In comparison with the spectra in displaced Morse oscillators, when the pump pulse is strong, many peaks appear on the spectra in the predissociation case, because of the reduction of population in the e state through the diabatic coupling. The time evolution of the wavepacket shows the interplay of the predissociation and laser excitation in a dissipative environment.

Acknowledgements

References

[1] A.D. Bandrauk, M.L. Sink, J. Chem. Phys. 74 (1981) 1110.
[2] M. Shapiro, H. Bony, J. Chem. Phys. 83 (1985) 1588.
[3] C. Wunderlich, H. Figger, T.W. Hänsch, Chem. Phys. Lett. 256 (1996) 43.
[4] P. Schwendner, F. Seyl, R. Schinke, Chem. Phys. 217 (1997) 233.
[5] M.S. Child, R. Lefebvre, Chem. Phys. Lett. 55 (1978) 213.
[6] M.S. De Vries, N.J.A. Van Veen, M. Hutchinson, A.D. De Vries, Chem. Phys. 51 (1980) 159.
[7] H. Guo, J. Chem. Phys. 99 (1993) 1685.
[8] Y. Wang, C.X.W. Qian, J. Chem. Phys. 100 (1994) 2707.
[9] Y. Tanimura, S. Mukamel, J. Phys. Soc. Jpn. 63 (1994) 66.
[10] Y. Tanimura, Y. Maruyama, J. Chem. Phys. 107 (1997) 1779.
[11] B.R. Mollow, M.M. Miller, Ann. Phys. 52 (1969) 464.
[12] P.L. Knight, P.W. Milonni, Phys. Rep. 66 (1980) 21.
[13] H. Tsunetsugu, E. Hanamura, J. Phys. Soc. Jpn. 55 (1986) 3636.
[14] Y. Tanimura, R. Kubo, J. Phys. Soc. Jpn. 58 (1989) 101.
[15] Y. Tanimura, P.G. Wolynes, Phys. Rev. A43 (1991) 4131.
[16] Y. Tanimura, P.G. Wolynes, J. Chem. Phys. 96 (1992) 8485.
[17] E. Wigner, Phys. Rev. 40 (1932) 749.
[18] R. Kubo, J. Phys. Soc. Jpn. 19 (1964) 2127.
[19] Y. Tanimura, S. Mukamel, J. Chem. Phys. 101 (1994) 3049.
[20] M. Raab, G. Honing, W. Demetröder, C.R. Vidal, J. Chem. Phys. 74 (1985) 4370.
[21] W. Weickenmeier, U. Diemer, M. Wahl, M. Raab, W. Demtröder, W. Müller, J. Chem. Phys. 82 (1985) 5354.
[22] P. Meystre, M. Sargent III, Elements of Quantum Optics, 2nd ed. (Springer, New York, 1991).